

# The Crystal Structure and Ionic Conductivity Properties of $K_2ZnGe_2O_6$

Jekabs Grins and Per-Erik Werner\*

Department of Inorganic and Structural Chemistry, Arrhenius Laboratory, University of Stockholm, S-106 91 Stockholm, Sweden

Grins, J. and Werner, P.-E., 1989. The Crystal Structure and Ionic Conductivity Properties of  $K_2ZnGe_2O_6$ . – Acta Chem. Scand. 43: 11–14.

The crystal structure of  $K_2ZnGe_2O_6$  has been determined and refined directly from Guinier-Hägg powder diffraction data. A Rietveld refinement in space group  $C222_1$  [ $a = 9.7904(4)$ ,  $b = 6.3612(2)$  and  $c = 10.8078(4)$  Å] converged to  $R_F = 0.071$  and  $R_{wp} = 0.248$ . The structure exhibits a framework of corner-sharing  $ZnO_4$  and  $GeO_4$  tetrahedra, with chains of  $GeO_4$  tetrahedra parallel to the  $c$  axis interconnected by  $ZnO_4$  tetrahedra. The K atoms are located within channels in the framework. The ionic conductivity of  $K_2ZnGe_2O_6$  has been determined by impedance measurements and found to be  $7.9 \times 10^{-7} (\Omega \text{ cm})^{-1}$  at 600 K with an activation energy of  $E_a = 0.90$  eV. The ionic conductivity properties are discussed in relation to the structural information.

In connection with studies of the ionic conductivity in a series of silicates and germanates,<sup>1</sup> the crystal structure of  $K_2ZnGe_2O_6$  has been determined in order to correlate the ionic conductivity properties and the structural parameters. Because of difficulties in obtaining single crystals of the substance, the crystallographic study was performed by full-profile analysis of a Guinier-Hägg powder diffraction photograph.

The structure determination shows that the structure exhibits channels containing the  $K^+$  ions. The channels are furthermore interconnected by pathways wide enough for  $K^+$  ion interchannel migration. The  $K^+$  ion conductivity in  $K_2ZnGe_2O_6$  was determined by means of impedance measurements at a series of temperatures between 400 and 600 K. The ionic conductivity properties can be related, as discussed below, to features in the crystal structure.

## Experimental

The compound  $K_2ZnGe_2O_6$  was synthesized by solid-state reaction in air at ambient temperature. A pelletized mixture of appropriate amounts of dried *p.a.*  $K_2CO_3$ , ZnO and  $GeO_2$  was heated slowly to 1025 K and held at that temperature for 15 h. The material was then reground twice, pelletized, and heated for 15 h at 1025 K and for 15 h at 1125 K.

X-Ray powder diffraction photographs were taken using a focussing camera of Guinier-Hägg type with subtraction geometry and with strictly monochromated  $CuK\alpha_1$  radiation ( $\lambda = 1.5405981$  Å at 25°C). Finely powdered silicon [ $a = 5.430880(35)$  Å at 25°C]<sup>2</sup> was added as internal standard to the sample used to solve the indexing problem and to obtain accurate unit cell parameters. Step-scan intensi-

ties used for profile analysis were evaluated from a photograph taken without silicon but using lines from the sample as  $\theta$  standards. To avoid simultaneous appearance of front- and back-layer profiles and to diminish the background, single-coated film (CEA Reflex 15) was used.

All films were measured by means of a computer-controlled microdensitometer.<sup>3</sup> The slit opening of the collimator was  $0.040 \times 2.00$  mm, and the corresponding  $\theta$  step length was  $0.0286^\circ$  ( $2\theta$ ).

The impedance spectrometer used for the ionic conductivity measurements is described in Ref. 4.

## Structure determination and refinement

The powder pattern was indexed by the trial-and-error program TREOR.<sup>5</sup> The unit cell dimensions and figures of merit obtained are given in Table 1. The indexed pattern is listed in Table 2. Reflections with indices ( $hkl$ ) were ob-

Table 1. Crystal data.

Stoichiometry	$K_2ZnGe_2O_6$
Space group	$C222_1$
Z	4
F.W.	384.75
$a/\text{Å}$	9.7904(4)
$b/\text{Å}$	6.3612(2)
$c/\text{Å}$	10.8078(4)
$V/\text{Å}^3$	673.1
$d_{\text{calc}}/\text{g cm}^{-3}$	3.80
Cell figures-of-merit:	
$M_{20}$	156
$F_{30}$	261(0.0032,36)
$F_{50}$	193(0.0038,68)

\* To whom correspondence should be addressed.

Table 2. Observed and calculated  $2\theta$  values for the Guinier-Hägg powder diffraction pattern of  $K_2ZnGe_2O_6$  up to the 20th observed line.  $\Delta(2\theta) = 2\theta_{obs} - 2\theta_{calc}$ .  $\lambda = 1.5405981 \text{ \AA}$ .

(hkl)	$2\theta_{obs}$	$\Delta(2\theta)$	$d_{obs}$	$l/l_0$
(002)	16.396	0.006	5.402	115
(110)	16.609	0.003	5.333	101
(200)	18.114	0.007	4.893	141
(111)	18.533	-0.001	4.784	939
(112)	23.416	0.001	3.7960	22
(202)	24.522	0.005	3.6273	9
(020)	28.029	-0.002	3.1808	8
(021)	29.244	-0.002	3.0514	330
(113)	29.896	-0.009	2.9863	1000
(310)	30.765	-0.003	2.9039	674
(311)	31.887	-0.001	2.8043	337
(022)	32.655	0.013	2.7400	11
(004)	33.130	0.002	2.7018	60
(220)	33.574	0.000	2.6671	53
(221)	34.616	0.003	2.5982	141
(400)	36.692	0.005	2.4473	51
(114)	37.277	0.002	2.4102	121
(222)	37.580	0.003	2.3915	282
(204)	38.003	-0.005	2.3658	216
(313)	39.843	0.001	2.2607	174

served only for  $h+k = 2n$  and  $(00l)$  only for  $l = 2n$ , which is characteristic of space group  $C222_1$ .

A three-dimensional Patterson function was calculated from 129 integrated intensities with indices corresponding to the most close-lying calculated  $\theta$  values, thus disregarding the overlaps. From space group and density considerations it was concluded that there are four formula units in the unit cell. Therefore, the zinc atoms must occupy special positions. The Patterson map indicated a  $4(a)$  position to be occupied. The coordinates of the atoms were then derived by a combination of Fourier methods and structural considerations.

Full-profile Rietveld refinements of the structure were made with a local version of the program DBW3.2S, which is an updated version of the program described in Ref. 6. The DBW3.2S program, written for powder diffractometer data, has been modified to allow input of Guinier data. An important addition to the original program is therefore the possibility of using equal weights for all step-scan intensities below a chosen limit. As an aid in determining this limit, a weighting scheme is printed by the program. As proposed by Sonneveld and Visser<sup>7</sup> for Guinier data, the modified Lorentz function was used in the calculation of line profiles. The angular dependence of the peak full-width ( $2\theta$ ) at half-maximum was described by the usual quadratic equation in  $\tan \theta$ :

$$FWHM^2 = U \cdot \tan^2 \theta + V \cdot \tan \theta + W$$

where  $U$ ,  $V$  and  $W$  are parameters to be refined. The minimum and maximum values for the half-widths were found to be  $0.096$  and  $0.161^\circ$  ( $2\theta$ ), respectively. Step intensities in the  $2\theta$ -range  $5^\circ$  to  $83^\circ$  were used in the refine-

ments. The final profile refinement cycles involved the following parameters: 15 atomic coordinates, 3 combined absorption-temperature factors, 1 scale factor, 1 zero-point parameter, 3 cell parameters, 1 asymmetry and 2 half-width parameters. The refinement was terminated when all shifts in the parameters were less than 10% of the corresponding standard deviations. The final  $R$ -values,  $R_p = 0.173$ ,  $R_{wp} = 0.248$ ,  $R_B = 0.119$  and  $R_F = 0.071$ , were obtained for the positional parameters listed in Table 3. The calculated and observed patterns are shown in Fig. 1.

The structure is built up of corner-sharing  $ZnO_4$  and  $GeO_4$  tetrahedra (cf. Table 4), thus forming the framework shown in Fig. 2. Chains of corner-sharing  $GeO_4$  tetrahedra, parallel to the  $c$  axis, are interconnected by  $ZnO_4$  tetrahedra. As in the structure of  $Na_2ZnGeO_4$ ,<sup>8</sup> every  $ZnO_4$  tetrahedron has each of its four vertices in common with a  $GeO_4$  tetrahedron.

The  $K^+$  ions are located in a zig-zag fashion in channels parallel to the  $b$  axis. The  $K^+$  ions are irregularly coordinated by nine oxygen atoms at distances of  $2.67$ – $3.38 \text{ \AA}$ . The channels are wide enough for  $K^+$  ion migration to be possible along a zig-zag path in the  $(010)$  direction. Pathways of width similar to that of the channels also exist

Table 3. Positional parameters of  $K_2ZnGe_2O_6$  with estimated standard deviations in parentheses.

Atom	Position	$x/a$	$y/b$	$z/c$
Zn	4(a)	0.6984(6)	0	0
Ge	8(c)	0.4884(4)	0.6603(5)	0.6101(3)
K	8(c)	0.3276(7)	0.1103(11)	0.6789(6)
O(1)	8(c)	0.3226(17)	0.2888(26)	0.4224(15)
O(2)	8(c)	0.5931(17)	0.8824(26)	0.6272(15)
O(3)	4(a)	0.9299(23)	0	0
O(4)	4(b)	0	0.0016(39)	1/4

Table 4. Selected interatomic distances ( $\text{\AA}$ ) with estimated standard deviations in parentheses.

<b><math>ZnO_4</math>-tetrahedron</b>			
2 Zn–O(1)	2.00(2)	O(1)–O(1)	3.17(4)
2 Zn–O(2)	1.87(2)	2 O(1)–O(2)	3.12(3)
		2 O(1)–O(2)'	3.21(3)
		O(2)–O(2)	3.13(4)
<b><math>GeO_4</math>-tetrahedron</b>			
Ge–O(1)	1.69(2)	O(1)–O(2)	2.91(3)
Ge–O(2)	1.76(2)	O(1)–O(3)	2.89(3)
Ge–O(3)	1.76(1)	O(1)–O(4)	2.88(2)
Ge–O(4)	1.83(2)	O(2)–O(3)	2.80(2)
		O(2)–O(4)	2.93(3)
		O(3)–O(4)	2.79(1)
<b><math>KO_9</math>-polyhedron</b>			
K–O(1)	2.76(2)	K–O(2)''	3.03(2)
K–O(1)'	2.99(2)	K–O(3)	3.25(2)
K–O(1)''	3.09(2)	K–O(4)	3.09(2)
K–O(2)	2.67(2)	K–O(4)'	3.38(1)
K–O(2)'	2.93(2)		

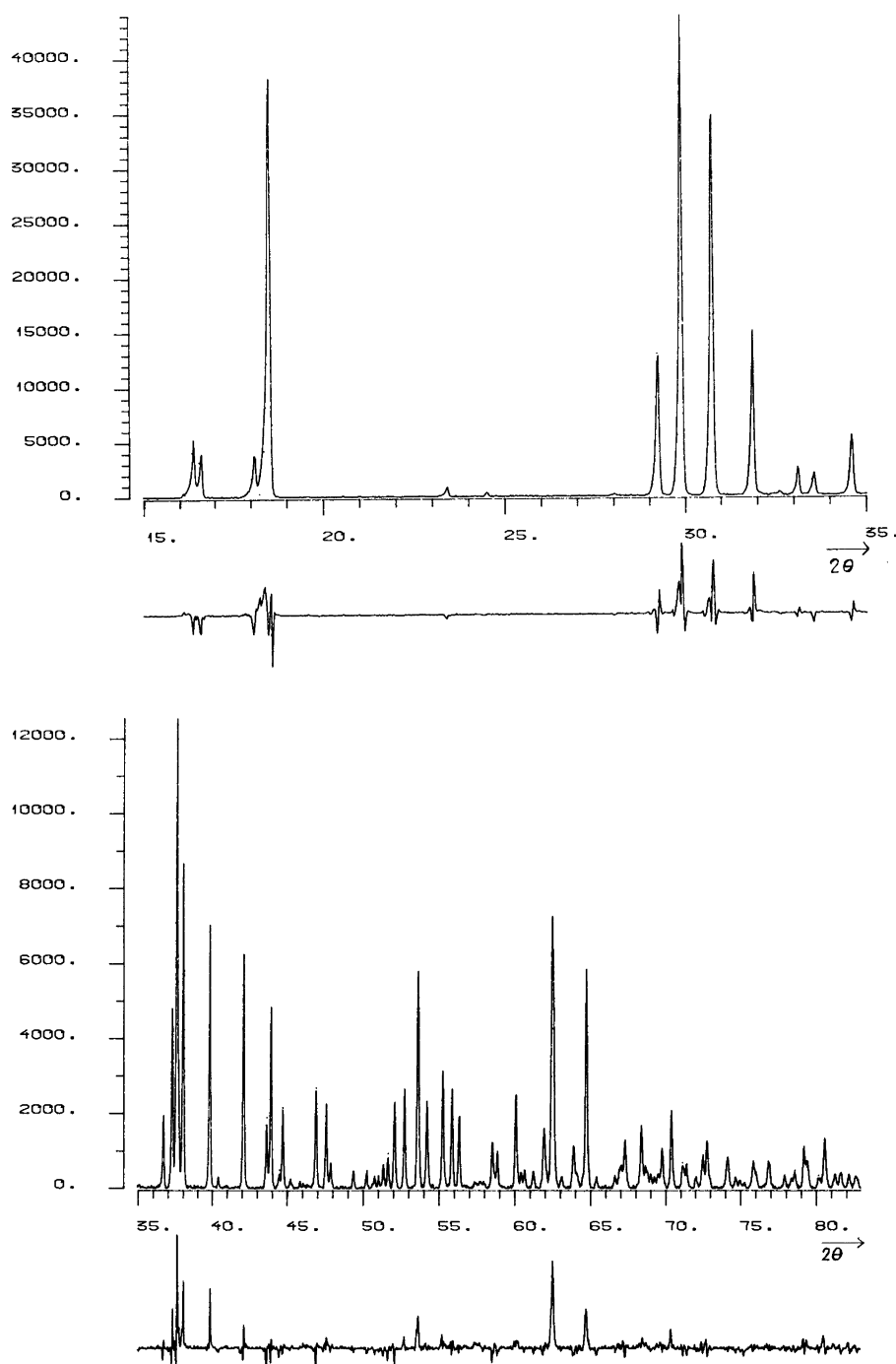


Fig. 1. Final Rietveld plot. In the upper portion, the observed data are shown as a solid line. Calculated intensities are shown as dots. The lower portion is a plot of the difference, i.e. observed minus calculated.

between the channels. The approximate directions of these pathways are indicated by the small arrows in Fig. 3, in which a part of the structure surrounding the K<sup>+</sup> ions is shown. The possible pathways for K<sup>+</sup> ion migration are also shown in Fig. 4 as lines connecting the K<sup>+</sup> ion positions. From a structural point of view, K<sup>+</sup> ion migration can thus be expected to occur in three dimensions.

### Ionic conductivity

The ionic conductivity of K<sub>2</sub>ZnGe<sub>2</sub>O<sub>6</sub> was determined by means of impedance measurements. The samples used in the measurements were 1–2 mm thick sintered disks with a diameter of 6 mm. Blocking electrodes were applied by evaporating gold onto the disks. The impedance was recorded as a function of frequency at six different temperatures between 400 and 600 K in a series of heating–cooling runs. The reproducibility was checked by measure-

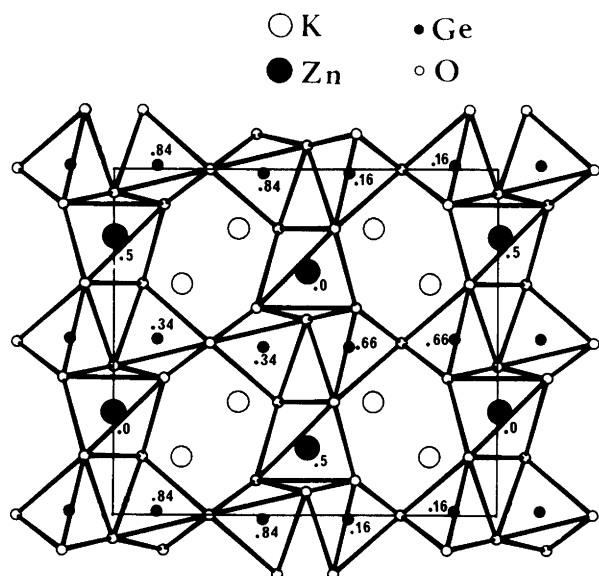


Fig. 2. The structure of  $K_2ZnGe_2O_6$  projected on the  $ac$  plane.

ments on several samples, and the agreement was found to be good. The ionic conductivity was calculated from the intercept of the semicircular arc obtained in complex impedance plots.

The conductivity was found to show Arrhenius-type behaviour:

$$\ln(\sigma_T) = \ln(\sigma_0) = E_a/kT.$$

The activation energy and the pre-exponential factor obtained were  $E_a = 0.90 \pm 0.02$  eV and  $\ln(\sigma_0) = 4.33 \pm 0.20$  ( $\Omega$  cm/K) $^{-1}$ , respectively. The conductivity at 600 K is  $9.7 \times 10^{-7}$  ( $\Omega$  cm) $^{-1}$ .

The ionic conductivity in  $K_2ZnGe_2O_6$  is thus rather limited. The channels in the (010) direction and the pathways

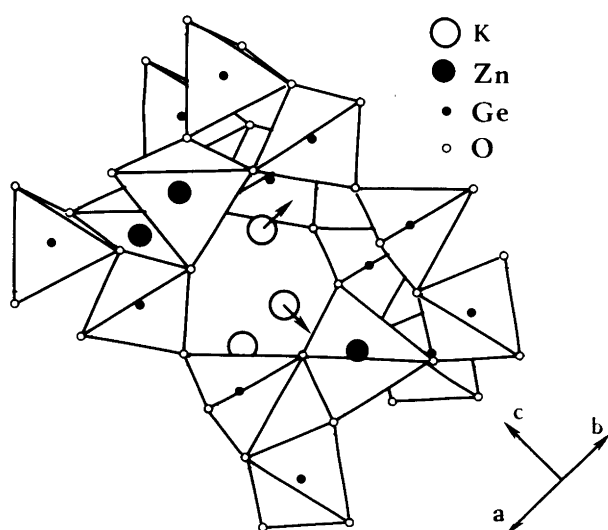


Fig. 3. A drawing of a part of the  $K_2ZnGe_2O_6$  structure showing the arrangement of  $ZnO_4$  and  $GeO_4$  tetrahedra around the K atoms located in one of the channels along the  $b$  axis. Possible diffusion pathways for  $K^+$  are indicated by arrows.

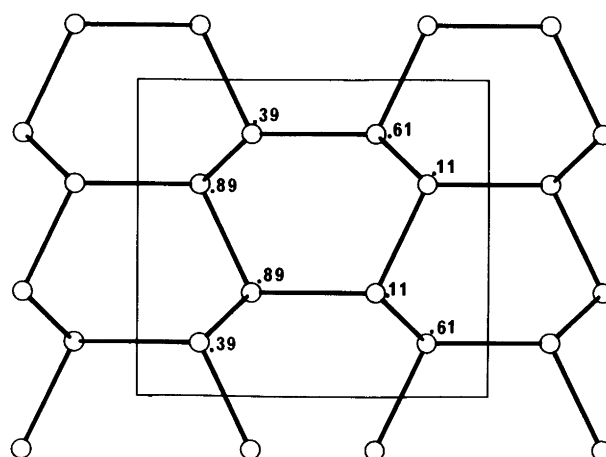


Fig. 4. The K atom positions in the unit cell of the  $K_2ZnGe_2O_6$  structure. The K atom positions that are connected by pathways large enough to allow  $K^+$  ion migration are connected by thick lines.

connecting these channels are wide enough for  $K^+$  ion migration. The  $K^+$  [8(c)] site is, however, fully occupied. This excludes a regular vacancy mechanism for the ionic conductivity. The channels and interchannel pathways are furthermore found to be relatively narrow and the  $K^+$  arrangement rather dense, with  $K^+ - K^+$  distances of 3.7–3.9 Å. This crowding of the  $K^+$  ions may prevent interstitial sites from becoming populated without a severe displacement of the surrounding  $K^+$  ions that occupy regular sites. The creation of interstitials would consequently be energetically unfavourable. The high activation energy observed for the ionic conductivity may accordingly be interpreted as being caused by the full occupancy of the  $K^+$  [8(c)] sites and by a high activation energy required to create interstitials/vacancies.

*Acknowledgements.* We wish to thank Dr. M. Nygren for his interest in this work and for many fruitful discussions.

This work has received financial support from the Swedish Natural Science Research Council.

## References

1. Frostäng, S., Grins, J. and Nygren, M. *Chem. Scr.* 28 (1988) 107.
2. Hubbard, C. R., Swanson, H. E. and Mauer, F. A. *J. Appl. Crystallogr.* 8 (1975) 45.
3. Johansson, K.-E., Palm, T. and Werner, P.-E. *J. Phys. E* 13 (1980) 1289.
4. Hörlin, T. *Chem. Scr.* 25 (1985) 270.
5. Werner, P.-E., Eriksson, L. and Westdahl, M. *J. Appl. Crystallogr.* 18 (1985) 367.
6. Wiles, D. B. and Young, R. A. *J. Appl. Crystallogr.* 14 (1981) 149.
7. Sonneveld, E. J. and Visser, J. W. *J. Appl. Crystallogr.* 8 (1975) 1.
8. Kuzmin, E. A., Ilyukhin, V. V. and Belov, N. V. *Soviet Phys. Crystallogr.* 13(6) (1969) 848.

Received March 18, 1988.